Pergamon

Int. J. Solids Structures Vol. 32, No. 24, pp. 3589–3602, 1995
Elsevier Science Ltd
Printed in Great Britain
0020–7683/95 $9.50 + .00

0020–7683(95)00020–8

ON THE ECCENTRICITY FACTOR IN THE PROGRESSIVE CRUSHING OF TUBES

A. A. SINGACE,† H. ELSOBKY and T. Y. REDDY
Mechanical Engineering Department, UMIST, P.O. Box 88, Manchester M60 1QD, U.K.

(*Received* 29 *March* 1994; *in revised form* 27 *December* 1994)

Abstract—The analysis of an axially compressed circular tube deforming in progressive axi-symmetric folds carried out by Wierzbicki *et al.* [(1992) *Int. J. Solids Structures* **29**, 3269–3288] assumes an eccentricity factor relating the inward and outward parts of the folds. This factor was arbitrary and was not derived from the analysis. The present work re-examines the problem and produces a value for the eccentricity factor which conforms with the experimental findings. Values of the critical angles required for the formation of the inward and outward folds obtained from the analysis were substantiated by those obtained from experiments.

1. INTRODUCTION

The classical problem of cylinders and tubes subjected to gross axial compression is of technological interest, for example in the design of impact energy absorbing elements. Numerous papers have been published on various aspects of the problem. An excellent review of the literature on the plastic crushing behaviour of a tube has been given by Jones (1989). When a short cylindrical tube is axially compressed beyond the elastic range (Mallock, 1908; Coppa, 1962; Horton *et al.*, 1966; Allan, 1968; Johnson, 1972; Johnson *et al.*, 1977; Sobel and Newman, 1980; Andrews *et al.*, 1983), it will progressively fold into either axisymmetric concertina (ring) type folds or diamond shaped folds depending on its diameter to wall thickness (D/t) ratio. Relatively thicker tubes generally deform into axisymmetric folds and thinner tubes exhibit diamond type folds. Some tubes start deforming into axisymmetric folds but then revert to a diamond mode as collapse progresses. The reverse of such a phenomenon has not been observed. This study will focus only on tubes deforming into concertina folds.

The first fold almost always forms at one of the two ends of the tube and is facilitated by a radially outward movement, the magnitude of which is a function of the distance from the edge of the tube. A plastic bending hinge (or more correctly a plastic zone) appears at a certain distance from the end of the tube. This distance is dictated by the tube geometry and is usually of the order of $\sqrt{Rt}$ where R is the radius of the tube. In a fixed boundary condition, a tube with welded ends for instance, a plastic bending hinge will also appear near the fixed edge. On the other hand, no such edge hinge appears in the formation of a fold for simply supported tubes. In either case, the ends of the tube are radially restrained.

For a tube compressed between two flat plates, a semi-free boundary condition exists. In the initial stages of compression, the tube behaves as if its edges are fixed because of the square end faces and the influence of friction between the surfaces in contact. As loading progresses, radially inward forces are generated by the hoop expansion of the radially outward moving parts of the tube. When these forces are large enough to overcome the forces due to friction between the tube and the platen, the edge region undergoes radially inward movements. The mechanism of the initiation of the first fold is the same regardless of the edge conditions. However, the development of the first fold and hence the load–compression history during the folding process will depend on the edge conditions. Nevertheless, the formation of the subsequent folds and the further progressive crush behaviour

† Permanent address: Mechanical Engineering Department, College of Engineering, University of Bahrain, P. O. Box 32038, Manama, Bahrain.

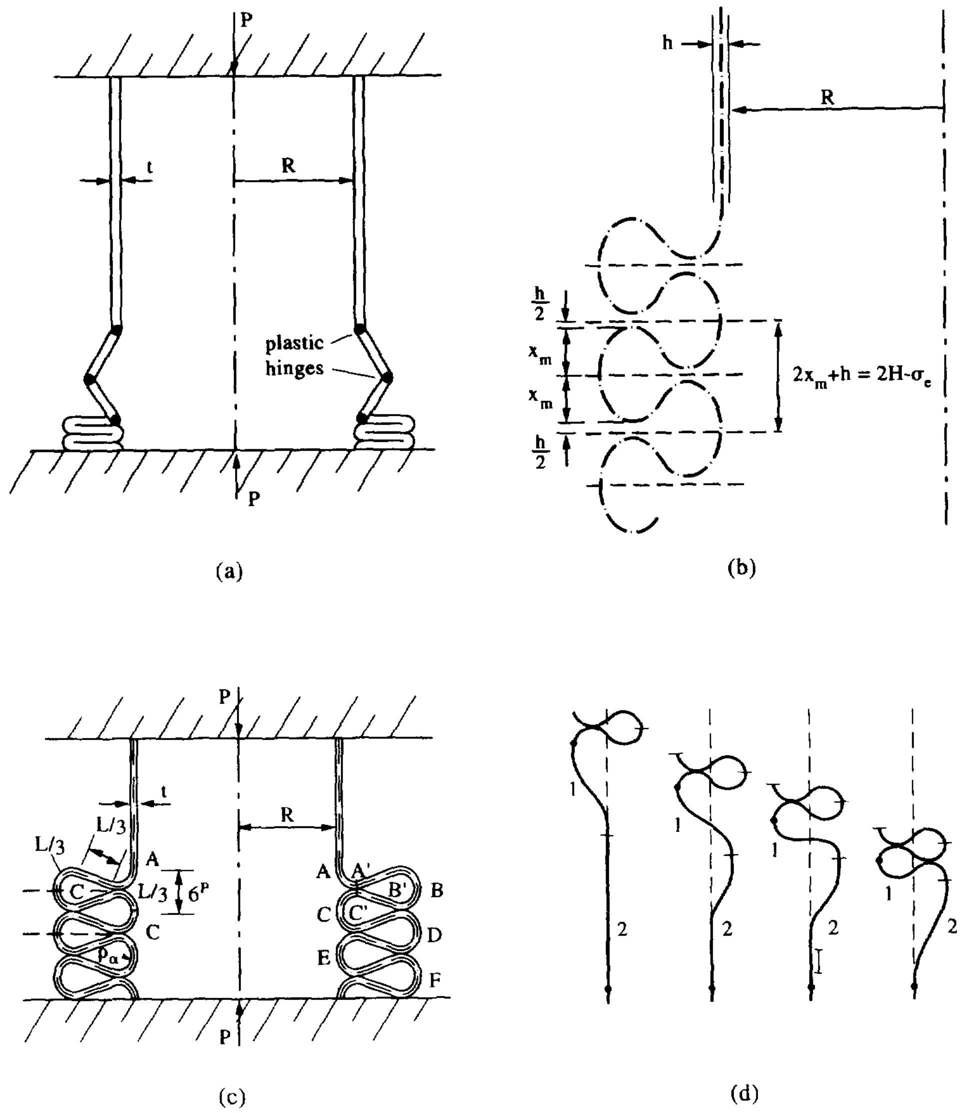

Fig. 1. Different failure mechanisms proposed to model the concertina mode due to: (a) Alexander (1960); (b) Abramowicz and Jones (1986); (c) Grzebieta (1990); and (d) Wierzbicki *et al.* (1992).

of the tube become independent of the edge conditions after the first fold has completely flattened.

In any given fold, the outer portion of a typical region of the tube's wall bound by two successive circumferential plastic hinges experiences radially outward movement, while the inner portion undergoes radially inward movement, unless such movements are constrained as described by Ahmed (1990). In an unrestrained tube subjected to axial loading and deforming in a concertina mode, a larger portion of a typical fold exhibits an outward motion than that moving inwards.

In the early analysis by Alexander (1960) of an axially compressed tube, the material was assumed to be rigid perfectly-plastic, and the tube was assumed to undergo axisymmetric folding. Alexander considered a general fold, other than the one near the edge of the tube [see Fig. 1(a)], and produced an upper bound solution for the mean crushing load assuming that folding is facilitated by a kinematic mechanism with three circumferential plastic hinges. The region between the extreme hinges was assumed to move either completely outwards or completely inwards, exhibiting plastic stretching (or compression) in the hoop direction. By minimizing the work carried out to deform one fold, the distance between two adjacent plastic hinges was obtained as $\sim\sqrt{Dt}$. Amdahl and Soreide (1981) used rate equations for the outward folding mechanism of Alexander's model and derived the load–deflection history during a fold cycle. As a perfectly straight tube was considered to start with, the load for initiating the fold turns out to be infinite in this analysis.

A more rigorous analysis by Andronicou and Walker (1981), where the von Mises yield condition was employed, considering the interaction between axial bending and circumferential stress resultants for the formation of the first hinge. In this study, the fully plastic bending moment and the distance between plastic hinges become dependent on the axial force. Simply supported as well as built-in edge conditions were considered. It is shown that the initial peak load is independent of the edge condition and that the load–tube shortening histories are different for the two edge conditions. At a given deformation, a tube with fixed edges has three bending hinges in the folding mechanism and hence requires a larger compressive force than that needed by an identical simply supported tube wherein only two circumferential plastic hinges form.

A more realistic radially outward folding mechanism was formulated by Abramowicz and Jones (1984, 1986), Wierzbicki and Bhat (1986) and Grzebieta (1990). In the first study, Abramowicz and Jones assumed that the region between the plastic hinges which undergoes hoop expansion in Alexander's model will have two equal parts of the same curvature but of opposite sense, Fig. 1(b). Only the calculation of the mean load was addressed in their analysis. Wierzbicki and Bhat employed a moving hinge mechanism starting from each end of the fold length. Grzebieta, however, assumed that the two curved regions are separated by a straight region where each region is one-third of the fold leg length, see Fig. 1(c). Considering the interaction between the axial bending and the circumferential stretching stress resultants, Grzebieta obtained the mean crushing load as well as the load–compression history during one fold cycle. In all these models, only radially outward folding is assumed.

A more recent study of the problem was carried out by Wierzbicki *et al.* (1992) where a new approach to the representation of the concertina collapse mode of tubes was introduced. The authors used a model based on the assumption that crushing progresses by virtue of instantaneous formation of three stationery plastic hinges leading to a fold comprised of two elements of equal lengths. As the fold develops, the mechanism allows both inward and outward radial displacements of the tube generator according to a certain ratio. This ratio, denoted by m, represents a geometric eccentricity factor which has not been introduced in earlier publications. The load–compression history as well as the mean load have been analysed. This model will be discussed further in the following section.

The introduction of the eccentricity factor, m, in the analysis leads to the successful qualitative reproduction of many of the features characterizing the physical behaviour of tubes folding in a concertina mode. However, in the analysis developed by Wierzbicki *et al.* (1992), the value of m was arbitrary and indeterminate. This drawback withheld further clarification of additional characteristics which was not explicitly mentioned in their paper. These include in particular the critical inclination angles of the folding elements corresponding to inward and outward folds. However, Wierzbicki *et al.* (1992) carried out the analysis for arbitrary values of m and proceeded to develop a superfolding element model for the problem.

In this paper, using a rigid perfectly-plastic material, Wierzbicki's stationary plastic hinge model is taken one step further and, following the same basic procedure, definite values for the eccentricity factor, m, and the critical angles for the formation of the inward and outward folds are derived. The value of m obtained from the analysis agrees with the experimental observations. Some thoughts on the initial folding of a tube that are applicable to all edge conditions are presented. The scope of this paper is confined to the derivation and discussion of the eccentricity factor, although it can be extended further to obtain the load–displacement history during a fold cycle.

2. DETAILS OF THE MODEL

2.1. *Initiation of folding process*

Understanding the process of formation of the first fold is crucial for modelling subsequent folds. While a rigorous analysis of the formation of the first fold will not be

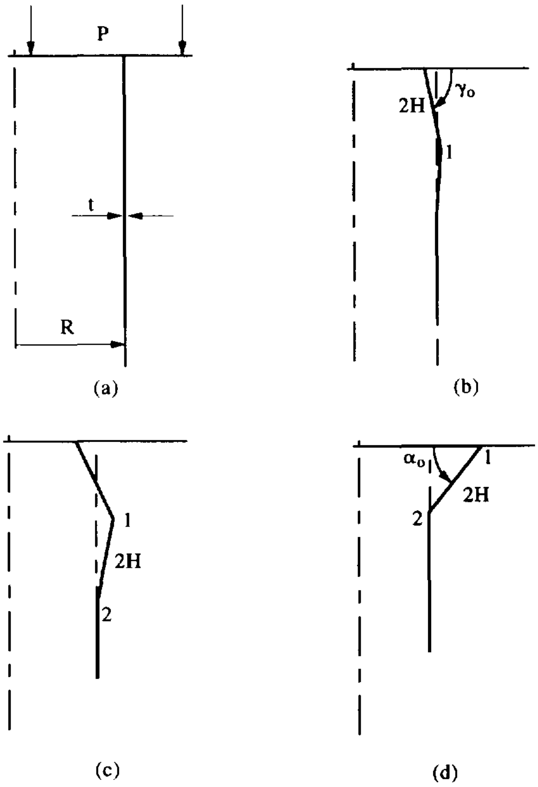

Fig. 2. The development of the initial (outward) fold in an undeformed tube: (a) undeformed tube; (b) start of the first fold; (c) intermediate stage in the first fold; and (d) completion of first outward fold, critical position for the first inward fold.

addressed in the present study, this main physical feature, based on experimental observations, will be used to establish the continuity of the crushing process with each subsequent fold. Experiments show that the first fold will always form with an outward buckle. The process is depicted qualitatively in Fig. 2. Photographs of sectioned specimens (a typical one is portrayed in Fig. 3) were used to obtain the straight line segments that show how the formation of the first fold progresses. It is to be noted, however, that once the first fold has been formed, critical angles, α_o and β_o, necessary for the definition of the inward (see Fig. 4) and outward folds (see Fig. 5), respectively, will appear in the analysis of the concertina mode of failure.

Friction effects, and geometric and material imperfections, play an important role in the formation of the initial buckle. As the tube is compressed, its wall tends to move radially outwards, due to a Poisson effect and axial shortening; however, the radially outward sliding movement of the ends of the tube is resisted by virtue of frictional forces between the testing machine platens and the ends of the tube. This will result in the ends of the tube lagging behind the rest of the tube wall and hence the initiation of the first outward buckle. As the fold leg adjacent to the platen bends, it reaches a critical angle, γ_o, at which point a circumferential plastic hinge is created to facilitate axial bending and hence fold formation. Deformation continues with γ_o diminishing to zero while the second leg of the fold will acquire a rotation to reach a critical value α_o. As collapse progresses (i.e. $\gamma_o \to 0$), the end of the tube slides inwards from its initial position (thus undergoing compression) until it is completely flat, lying partly to the outside and partly to the inside of the tube generator. The fractional length of the leg to the outside of the tube generator is Wierzbicki's eccentricity factor m, mentioned earlier.

The minimum leg length for a concertina fold is what is usually termed the plastic fold length and is shown to be approximately equal to $\sqrt{Dt}$ by Alexander (1960). We represent this by H_{Alex}, and it is equivalent to $2H$ in this paper. The plastic fold length H_{Alex} has been

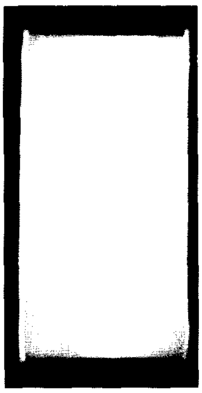

3

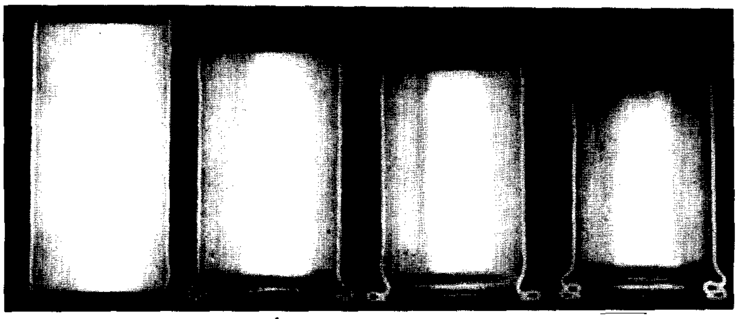

8 a b c d

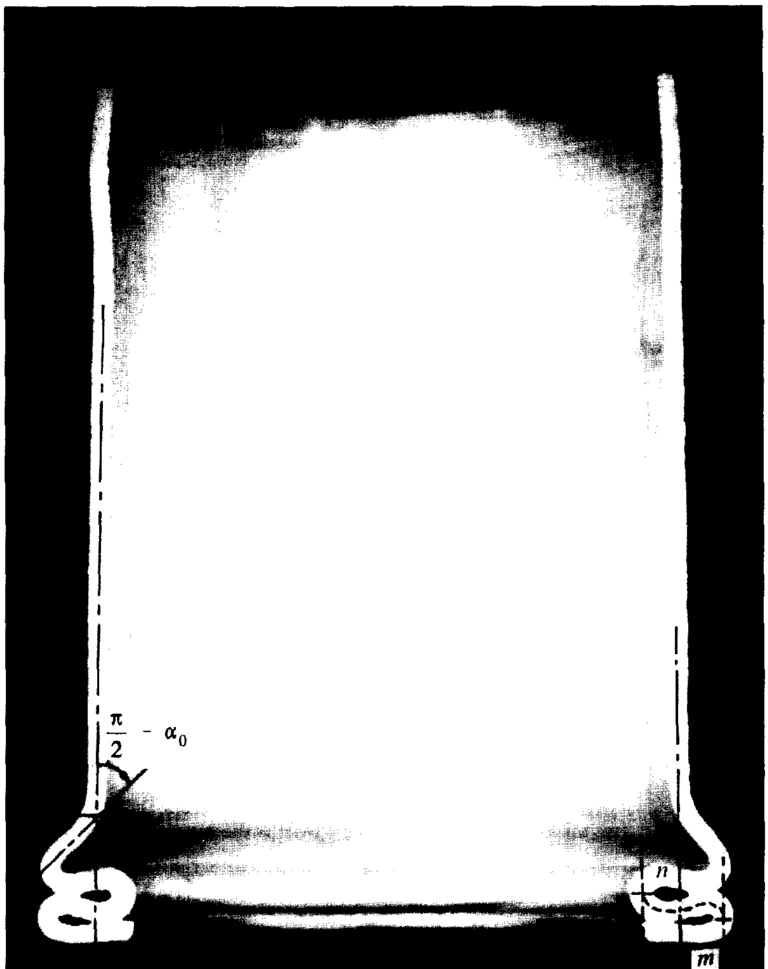

7

Fig. 3. Photographic view of the cross-section of a tube deformed to the critical position for the formation of the initial fold (outward).

Fig. 7. A photographic image of a tube, compressed up to the start of the second inward fold, used to obtain the values of m and α_0.

Fig. 8. Photographs showing the aluminium tube deformed up to the start of: (a) first outward fold; (b) first inward fold; (c) second outward fold; and (d) second inward fold.

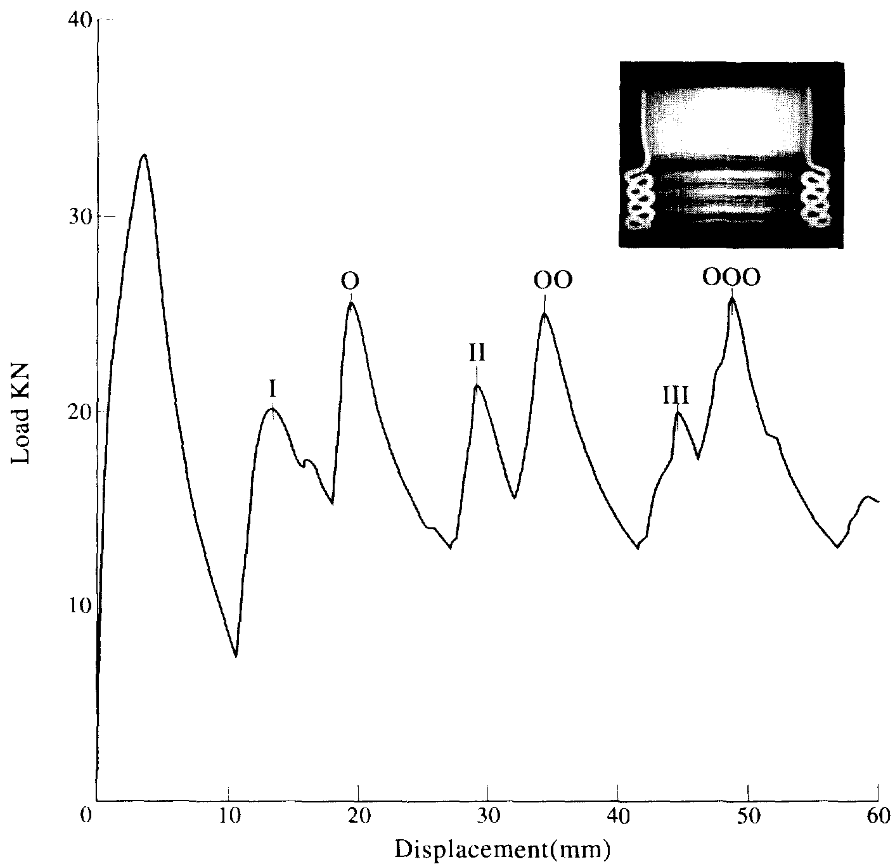

Fig. 6. Load–deflection curve for the axial compression test for an aluminium alloy tube of 50 mm outside diameter and 1.6 mm thickness (concertina mode). Inset is the tube compressed up to the fourth inward fold.

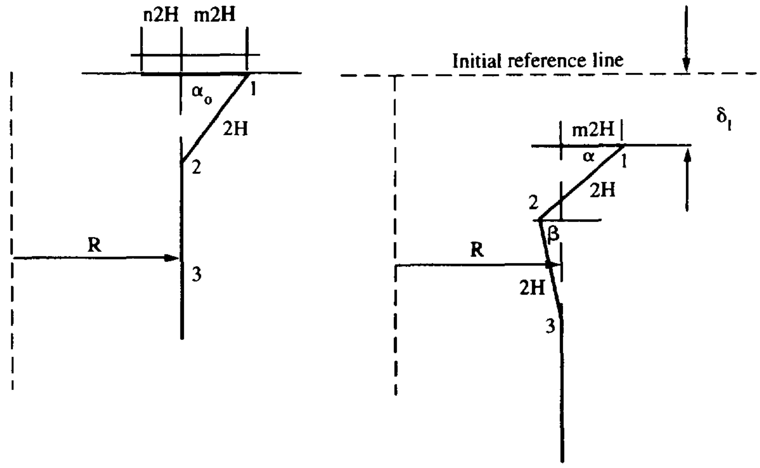

(a) (b)

Fig. 4. The formation and progression of the first inward fold (phase 1, second fold): (a) completion of the first fold; and (b) first phase of the second fold.

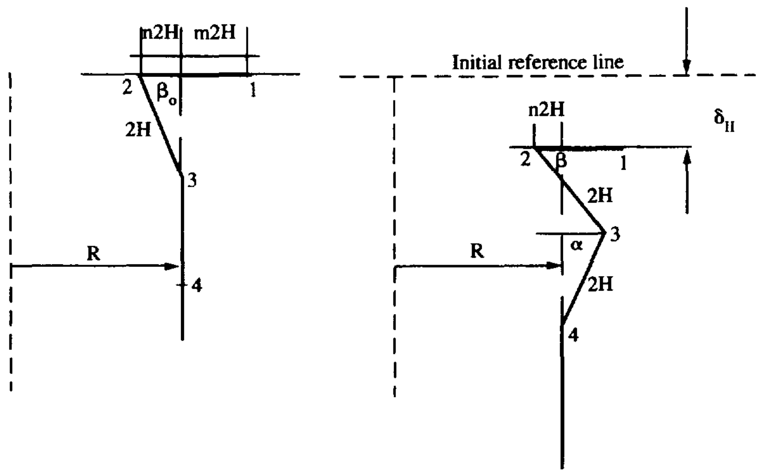

(a) (b)

Fig. 5. The transition between the first inward and the subsequent outward fold (phase 2, second fold): (a) completion of first phase of the second fold; and (b) second phase of the second fold.

verified experimentally and is the greatest strength of Alexander's analysis. Experimental measurements will be presented later.

2.2. *Subsequent folding*

As this end fold is completed, i.e. γ_o has diminished to zero, α_o, which characterizes the critical position for the next fold, is reached (Fig. 2). Further deformation is possible with the development of a new plastic hinge, point 3 in Fig. 4(a). The progressive collapse mechanism that causes deformations from this point onward are as described in detail by Wierzbicki *et al.* (1992). The angle α will diminish as the collapse progresses with the continuing deformation of this inward fold, with the completion of which another angle, associated with the formation of the next outward fold, will acquire a value of β_o. The growth of the second and the third folds is shown in Figs 4 and 5, respectively. The completion of an inward fold will result in the formation of the adjacent outward one and so on.

Global energy balance will be used and the sum of the plastic bending and stretching energies will be equated to the work done by the applied force to produce an expression for the mean crushing load P_m. The expression for P_m contains the fold length $2H$ and the eccentricity factor m, which are obtained through the minimization procedures.

3. ANALYSIS

3.1. *Bending energy*

In any given cycle of deformation representing a complete fold, the bending energy term is comprised of two parts; one associated with inward folding, controlled by a change in α (Fig. 4), and the other associated with outward folding, controlled by a variation in β (Fig. 5). The selection of representation of α and β is arbitrary as the two angles are interchangeable.

In the first phase of collapse, the two elements of the fold will be hinged at three circumferential sections, 1, 2 and 3 in Fig. 4(b). The eccentricity factor, m, is related to the critical angle, α_o, in this phase as follows:

$$\cos\alpha_o = m. \tag{1}$$

From the same figure, the compatibility relationship between α and β can be shown to be

$$\cos\beta = \cos\alpha - \cos\alpha_o$$
$$\cos\beta = \cos\alpha - m \tag{2}$$

and their rates are related by

$$\dot{\beta} = \frac{\sin\alpha\dot{\alpha}}{\sqrt{[1-(\cos\alpha - m)]}}. \tag{3}$$

The vertical displacement of the end of the tube, δ_1, defined from the reference position shown in Fig. 4(b), is given as

$$\delta_1 = 2H(1+\sin\alpha_o - \sin\alpha - \sin\beta) \tag{4}$$

and its rate obeys the equation:

$$\dot{\delta}_1 = -2H(\cos\alpha\dot{\alpha} + \cos\beta\dot{\beta}). \tag{5}$$

The rate of bending energy, $\dot{E}_b$, is given by:

$$\dot{E}_b = \sum_i 2\pi R_i M_o |\dot{\theta}_i|, \tag{6}$$

where $M_o = \sigma_o t^2/4$ is the fully plastic bending moment per unit circumferential length, σ_o is yield stress and t is the tube thickness. R_i and $\dot{\theta}_i$ are radial distance and the relative rates of rotation, respectively, at the ith hinge. These are given as

$$\dot{\theta}_1 = \dot{\alpha} \qquad R_1 = R+2mH$$
$$\dot{\theta}_2 = \dot{\alpha}+\dot{\beta} \qquad R_2 = R+2mH-2H\cos\alpha$$
$$\dot{\theta}_3 = -\dot{\beta} \qquad R_3 = R. \tag{7}$$

Thus rate of bending energy in the first phase becomes

$$\dot{E}_b^{I} = 2\pi M_o\{(R+2mH)|\dot{\alpha}| + (R+2mH-2H\cos\alpha)|\dot{\alpha}+\dot{\beta}| + R|\dot{\beta}|\}. \tag{8}$$

Using eqns (2) and (3), eqn (8) can be integrated over the duration of the folding cycle and the bending energy will be obtained. For this first phase of the folding cycle, α will vary from α_o to 0, while β changes from $\pi/2$ to β_o. Because it is a single-degree-of-freedom system, one of the two angles could be used as the control parameter to represent the whole system. Representing this first phase of the fold by α, the bending energy is given by:

$$E_b^I = 4\pi M_o\{(R+2mH)\alpha_o + H\sin\alpha_o - H[\sqrt{(2m-m^2)}-1] + R\sin^{-1}(1-m)\}. \tag{9}$$

During the second phase of folding (see Fig. 5) the eccentricity is defined as $n = 1-m$ and the radii of the plastic hinges are not equal to those in the first phase. Similarly to the first phase, the eccentricity factor, n, is related to the critical angle β_o as follows:

$$\cos\beta_o = 1-m = n. \tag{10}$$

From Fig. 5, geometric compatibility produces the relationship between α and β as

$$\cos\beta = \cos\alpha + n \tag{11}$$

and their rates obey the equation

$$\dot{\alpha} = \frac{\sin\beta\dot{\beta}}{\sqrt{[1-(\cos\beta-n)]}}. \tag{12}$$

The end shortening of the tube in this phase is defined as [see Fig. 5(b)]:

$$\delta_2 = 2H(1+\sin\beta_o - \sin\beta - \sin\alpha) \tag{13}$$

and its rate is given as:

$$\dot{\delta}_2 = -2H(\cos\beta\dot{\beta} + \cos\alpha\dot{\alpha}). \tag{14}$$

For this phase, θ_i and R_i in eqn (6) can be written as

$$\begin{aligned} \dot{\theta}_1 &= \dot{\beta} & R_1 &= R-2nH \\ \dot{\theta}_2 &= \dot{\beta}+\dot{\alpha} & R_2 &= R+2H\cos\alpha \\ & & &= R-2nH+2H\cos\beta \\ \dot{\theta}_3 &= -\dot{\alpha} & R_3 &= R \end{aligned} \tag{15}$$

and the rate at which the bending energy is dissipated, i.e. eqn (8), can be written as

$$\dot{E}_b^{II} = 2\pi M_o\{(R-2nH)|\dot{\beta}| + (R-2nH+2H\cos\beta)|\dot{\alpha}+\dot{\beta}| + R|\dot{\alpha}|\}. \tag{16}$$

Considering the angular variation in β as the control angle and integrating between β_o and 0, the bending energy in the second phase is given by the expression:

$$E_b^{II} = 4\pi M_o\{(R-2(1-m)H)\beta_o + H\sin\beta_o + H(\sqrt{1-m^2}-1) + R\sin^{-1}(m)\}. \tag{17}$$

The total bending energy E_b for the full fold is found by summing eqns (9) and (17). Hence:

$$\begin{aligned} E_b = 4\pi M_o\{&([R+2mH]\alpha_o + H\sin\alpha_o - H\sqrt{(2m-m^2)} + R\sin^{-1}(1-m)) \\ &+ ([R-2(1-m)H]\beta_o + H\sin\beta_o + H\sqrt{(1-m^2)} + R\sin^{-1}(m))\}. \end{aligned} \tag{18}$$

The critical angles, α_o and β_o, can be replaced by the eccentricity factor, m, from the geometrical relations

$$\cos\alpha_o = m \quad \text{and} \quad \sin\alpha_o = \sqrt{(1-m^2)}$$
$$\cos\beta_o = 1-m \quad \text{and} \quad \sin\beta_o = \sqrt{(2m-m^2)}. \tag{19}$$

The expression for E_b can be written as

$$E_b = 4\pi M_o\{([R+2mH]\cos^{-1}m+2H\sqrt{(1-m^2)}+R\sin^{-1}(1-m)) + ([R-2(1-m)H]\cos^{-1}(1-m)+R\sin^{-1}(m))\}. \tag{20}$$

Thus, the bending energy is a function of the geometric parameters R, t and H as well as the eccentricity parameter m.

3.2. *Membrane energy*

The membrane energy terms for the first and the second phases are the same as given by Wierzbicki *et al.* (1992). These are given below for completeness. For the first phase, the first term is

$$E_m^I = 8\pi N_o H^2(1-m). \tag{21}$$

The second term is given by

$$E_m^{II} = 8\pi N_o H^2 m. \tag{22}$$

By summing eqns (21) and (22), the total membrane energy term is determined as

$$E_m = E_m^I + E_m^{II} = 8\pi N_o H^2. \tag{23}$$

Unlike the bending energy term, the membrane energy term is independent of the parameter m.

3.3. *Expressions for* P_m, m *and* H

The total work done by the mean crushing load P_m acting over the two phases of compression is P_m. $4H$. The mean crushing load is calculated from balancing global energy such that

$$P_m 4H = E_b + E_m. \tag{24}$$

Setting $\lambda = R/H$, the normalized mean crushing load can written as

$$\frac{P_m}{M} = \pi\{(\lambda+2m)\alpha_o+\sin\alpha_o-\sqrt{(2m-m^2)}+\lambda\sin^{-1}(1-m) + (\lambda-2(1-m))\beta_o+\sin\beta_o+\sqrt{(1-m^2)}+\lambda\sin^{-1}m+8(R/\lambda t)\}, \tag{25}$$

or in terms of m,

$$\frac{P_m}{M_o} = \pi\{(\lambda+2m)\cos^{-1}m+\lambda\sin^{-1}(1-m)+(\lambda-2(1-m))\cos^{-1}(1-m) + 2\sqrt{(1-m^2)}+\lambda\sin^{-1}m+8(R/\lambda t)\}. \tag{26}$$

The parameters λ and m are as yet unknown. These can be obtained by minimizing P_m/M_o. Minimization of eqn (26) with respect to m produces the following expression:

$$\frac{-2m}{\sqrt{(1-m^2)}}-\frac{(1-m)}{\sqrt{(2m-m^2)}}+\cos^{-1} m+\cos^{-1}(1-m)=0 \tag{27}$$

which is independent of H. Solving eqn (27) using the Newton–Raphson numerical scheme gives $m = 0.65$. Similarly, minimizing eqn (26) with respect to H (noting that $\lambda = R/H$) gives the following expression:

$$-\frac{R}{H^2}\{\cos^{-1} m+\cos^{-1}(1-m)+\sin^{-1} m+\sin^{-1}(1-m)\}+\frac{8}{t}=0. \tag{28}$$

Taking into consideration the constant value of m defined by eqn (27), the folding length, H, is given by:

$$H=\sqrt{\left\{\frac{Rt}{8}[\cos^{-1} m+\cos^{-1}(1-m)+\sin^{-1} m+\sin^{-1}(1-m)]\right\}} \tag{29}$$

which reduces to

$$H=\sqrt{\left(\frac{\pi Rt}{8}\right)}. \tag{30}$$

This is the equivalent expression for H obtained by Alexander (1960).

Inserting the values of H and m into eqn (26), it can be seen that

$$\frac{P_m}{M_o}=4\pi^{3/2}\sqrt{\left\{\left(\frac{2R}{t}\right)+2\pi[m\cos^{-1} m-(1-m)\cos^{-1}(1-m)+\sqrt{(1-m^2)}]\right\}}$$

or

$$\frac{P_m}{M_o}=22.27\sqrt{\left(\frac{2R}{t}\right)}+5.632. \tag{31}$$

This expression for the mean collapse load is similar to that given by Wierzbicki *et al.* (1992) except for the constant 5.632.

4. EXPERIMENTAL RESULTS AND DISCUSSION

In order to verify the theoretical value of the eccentricity factor m and the relevant values of the critical angles α_o and β_o, a set of HT-30 aluminium alloy tubes, of 50.8 mm nominal outside diameter, 1.6 mm thickness and 101 mm in height, were crushed at a rate of 5 mm min^{-1}. All the tubes folded progressively in a concertina mode. The load–displacement curve of the concertina mode is characterized by alternate high and low load peaks. A typical curve is shown in Fig. 6. These peaks, marked O and I, correspond to the formation of outward and inward folds, respectively, and hence to the critical angles β_o and α_o. The objective of these experiments was to obtain the critical angles α_o and β_o by compressing the tubes to the required deformation level, i.e. up to the peak loads related to the formation of the folds. These tubes were sectioned (longitudinally) to carry out measurements to derive representative values for m, α_o and β_o. To obtain the value of m, the curved length of the folds on either side of the generator were measured after magnifying the image suitably (see Fig. 7). To measure α_o and β_o, a similar approach was followed in

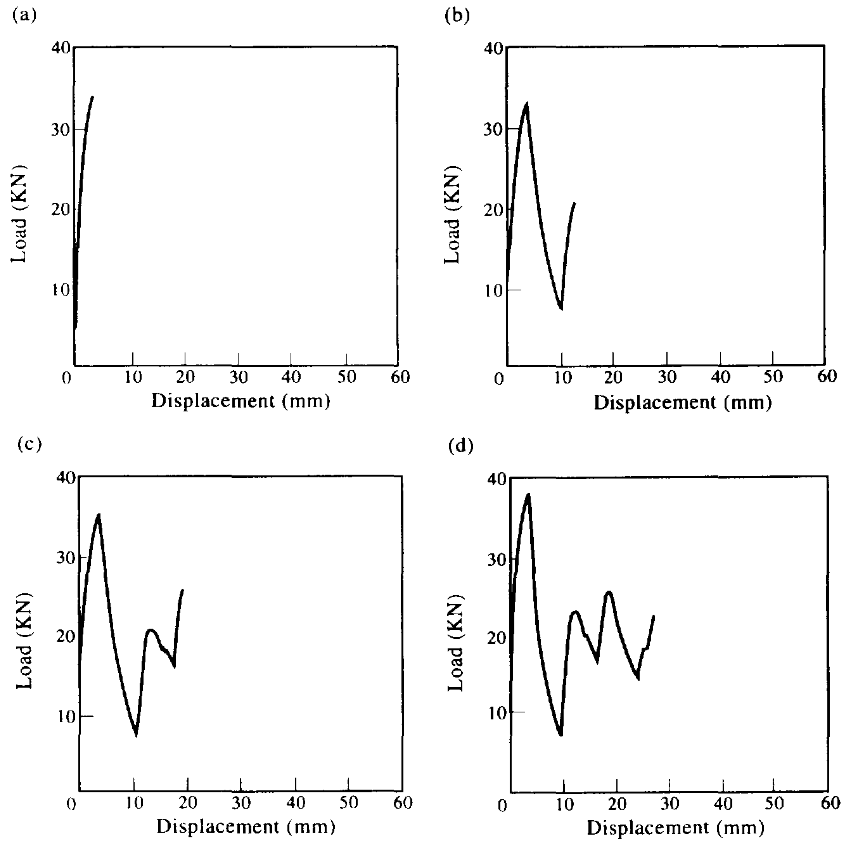

Fig. 9. The load deflection curves up to the start of: (a) first outward fold; (b) first inward fold; (c) second outward fold; and (d) second inward fold.

the relevant section of the tube. Figure 8 shows a photographic cross-sectional view of these tubes and the load displacement curves for the first four peaks are displayed in Fig. 9. The respective critical inclination angles from the experiments are listed in Table 1 along with those calculated using eqn (19), and it may be seen that there is a good agreement between the two. The value of γ_o measured from Fig. 3 is also shown in the Table. The values of m were measured for other HT-30 aluminium alloy tubes of different D/t ratios and were found to be nearly of constant magnitude. These results are shown in Table 2. The values of H are also shown in these tables and compared with the theoretical values given by eqn (28). Computation of m, α_o and β_o is possible due to the consideration of the variations in the value of the radial distances, R_p, at the plastic hinges during the formation of the folds.

Equation (26) is a function of m and λ and should be expected to produce two coupled equations from which m and H are to be determined; however, the differential operation

Table 1. Experimental and theoretical results for first four consecutive peaks

Peak (Fig. 9)	Measured angle (deg)	Theoretical critical angle (deg)	Peak load (kN)	End shortening (mm)	Measured value of m†	Fold length $2H$ (mm)
First (first outward fold)	$\gamma_o = 84$		34.30	3.321	—	—
Second (first inward fold)	$\alpha_o = 50$	49.62 Equation (1)	20.44	12.77	0.58	8.25
Third (second outward fold)	$\beta_o = 68$	69.38 Equation (10)	25.69	19.52	0.58	7.75
Fourth (second inward fold)	$\alpha_o = 49$	49.62 Equation (1)	22.06	27.265	0.59	8.5

† The theoretical value of m is 0.65, see eqn (27).

Table 2. Eccentricities and fold lengths for tubes of different mean diameter and thickness (D and t)

	D (mm):	22.5	23	48.5	49.2
	t (mm):	0.5	1.0	1.5	1.6
$2H$	Measured	3.17	4.38	8.15	8
(mm)	Theory, eqn (30)	4.2	6.0	10.78	11.1
m	Measured	0.60	0.63	0.62	0.59
	Theory, eqn (27)	0.65	0.65	0.65	0.65

$\delta(P_m/M_0)/\delta m = 0$ produces eqn (27) which is independent of H and which provides m directly. The value of m is also independent of the other geometrical parameters, namely R and t. Experimental measurements shown in Table 2 indicate that the eccentricity factor appears to be mildly dependent on the relative thickness of a tube. It should be expected that m also depends on the strain hardening characteristics of the tube material. If a strain hardening material model is considered, the equivalents of eqns (27) and (28) may become coupled.

In the present analysis, only the mean crushing load is discussed because the prime factor of interest is the eccentricity factor. Taking this procedure further and using energy rate equations instead of energy equations [following Wierzbicki *et al.* (1992), for example], the load–compression history during the folding process can be obtained.

The interaction of axial bending and membrane (hoop) stress resultants is not considered in this paper. A more rigorous analysis of the deformation using yield criteria [see Andronicou and Walker (1981) and Grzebieta (1990)], shows that, while there is little or no change in the thickness (with von Mises or with Tresca yield criteria, respectively) in the outward buckling region of the tube, the thickness of the tube changes in the inward buckling region. Consideration of such thickness changes produces a more complex expression for the bending energy dissipated and further complicates the expression for m and H. To maintain simplicity and to bring out the most salient feature of the problem, namely the eccentricity factor of Wierzbicki *et al.*'s model, this complication was felt unnecessary and hence the interaction effects are not included here.

5. CONCLUSIONS

The model proposed by Wierzbicki *et al.* (1992) for the collapse of a tube into the concertina mode is re-examined. The strength of their work was the introduction of the eccentricity factor, m, which, with reference to the tube generator, relates the inward and the outward parts of the fold. Nevertheless, m was arbitrary and could not be calculated from their analysis. The present analysis produces a value for m and consequently the critical angles required for the formation of the inward and outward folds. The present investigation does not include the analysis related to the initial fold, although some light has been shed on the development of the first buckle using the experimental observations. The values of m, α_0 and β_0 obtained from the analysis agree well with those obtained from the tests carefully carried out to measure the critical angles of the inward and outward folds. Further refinements should be possible with the use of flow rules which indicate the changes in the thickness at the plastic hinges.

REFERENCES

Abramowicz, W. and Jones, N. (1984). Dynamic axial crushing of circular tubes. *Int. J. Impact Engng* **2**, 263–281.

Abramowicz, W. and Jones, N. (1986). Dynamic progressive buckling of circular and square tubes. *Int. J. Impact Engng* **4**, 243–270.

Ahmed, R. (1990). Axial compression of thin metal tubes. M.Sc. Dissertation, UMIST, Manchester.

Alexander, J. M. (1960). An approximate analysis of the collapse of thin cylindrical shells under axial loading. *Q. J. Mech. Appl. Math.* **13**, 10–15.

Allan, T. (1968). Experimental and analytical investigation of the behaviour of cylindrical tubes subjected to axial compressive forces. *J. Mech. Engng Sci.* **10,** 182–197.

Amdahl, J. and Soreide, T. H. (1981). Energy absorption in axially compressed cylindrical shells with special reference to bulbous bows in collision. *Norwegian Maritime Res.* **4,** 2–11.

Andrews, K. R. F., England, G. L. and Ghani, E. (1983). Classification of the axial collapse of cylindrical tubes under quasi-static loading. *Int. J. Mech. Sci.* **25,** 687–696.

Andronicou, A. and Walker, A. C. (1981). A plastic collapse mechanism for cylinders under uniaxial end compression. *J. Const. Steel Res.* **1,** 23–34.

Coppa, A. P. (1962). Collapsible shell structures for lunar landing. General Electric Co. Report TIS R62SD9.

Grzebieta, R. H. (1990). An alternative method for determining the behaviour of round stocky tubes subjected to an axial crush load. *Thin-Walled Structures* **9,** 61–89.

Horton, W. H., Bailey, S. C. and Edwards, A. M. (1966). Nonsymmetric buckle patterns in progressive plastic buckling. *Exp. Mech.* **6,** 433–444.

Jones, N. (1989). *Structural Impact.* Cambridge University Press, Cambridge.

Johnson, W. (1972). *Impact Strength of Materials.* Edward Arnold, London.

Johnson, W., Soden, P. D. and Al-Hassani, S. T. S. (1977). Inextensional collapse of thin-walled tubes under axial compression. *J. Strain Anal.* **12,** 317–338.

Mallock, A. (1908). Note on the instability of tubes subjected to end pressure and on the folds in a flexible material. *Proc. R. Soc.* **A81,** 388–393.

Sobel, L. H. and Newman, S. Z. (1980). Plastic buckling of cylindrical shells under axial compression. *Trans. ASME, J. Press. Vess. Technol.* **102,** 40–44.

Wierzbicki, T. and Bhat, S. U. (1986). A moving hinge solution for axisymmetric crushing of tubes. *Int. J. Mech. Sci.* **28,** 135–151.

Wierzbicki, T., Bhat, S. U., Abramowicz, W. and Brodkin, D. (1992). Alexander revisited—a two folding elements model of progressive crushing of tubes. *Int. J. Solids Structures* **29,** 3269–3288.